Deep lung nodule detection using multi-resolution analysis on computed tomography images

Inbasakaran Govindan, Anitha Ruth Joseph Raj

Department of Computer Science and Applications, Faculty of Science and Humanities, SRM Institute of Science and Technology,
Vadapalani, India

Article Info

ABSTRACT

The lung nodule must be detected early because the patient's outcome can be enhanced following the lung cancer diagnosis. The candidate research proposed a novel computer-aided detection system based on multi-resolution technique (MRT) and local Gaussian distribution (LGD) methods to accurately identify and label the lung nodules in a computed tomography (CT) screening image. The research aimed to find all the potential nodule constructs, which combined wavelet and multiscale morphological analysis and then used the LGD method to calculate the Gaussian function parameters for each image block. Subsequently, we calculated the probability that each pixel belongs to a particular institute, which shall be used to achieve lung nodule segmentation reliably. After the segmentation, the research employed a convolutional neural network (CNN) variant to improve the detection performance further. The proposed method attained an accuracy of 0.9958, a sensitivity of 0.7899, a specificity of 0.9994 and an F1-score of 0.8651. The comparison with other methods shows that the proposed method had better detection accuracy than the different methods in terms of lung nodule detection.
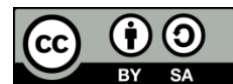
Corresponding Author:

Anitha Ruth Joseph Raj
Department of Computer Science and Applications, Faculty of Science and Humanities
SRM Institute of Science and Technology
Vadapalani, Chennai, India
Email: anithaj@srmist.edu.in

1. INTRODUCTION

In the global context, lung cancer remains the primary killer, which accounts for a considerable portion of the studies reporting cancer at an advanced stage with a poor survival rate [1]. Lung nodule identification at an early stage plays a vital role of signaling enhanced patient prognosis and appropriate treatment [2]. The nodule detection and segmentation requires computed tomography (CT) screening which has now become an essential tool for diagnosing lung cancer [3]. However, multiple factors limit the use of CT scans in diagnosis, and these include complexity and the number of images generated during the process, making classification of nodules by radiologists a difficult task [4]. Thus, it requires an automated computer-aided detection (CAD) system to improve the diagnostic accuracy and possible intervention plans [5].

Other challenges involved in the classification of nodules are; morphological variations seen in CT images, image noise or even overlapping structures of the lungs [6], [7]. Based on these challenges, CAD systems have become indispensable tools to support radiologists in decision making and analysis [8]. Therefore, there is an urgent need to develop a reliable segmentation method where the nodules in the lung region can be accurately localized and segmented to help in their classification or identification [9].

In response to this need, the goal of this research is to establish a CAD system for lung nodule detection in CT screening images using the multi-resolution technique (MRT) and the local Gaussian distribution (LGD) method. The multiscale morphological analysis (MMA) will first detect possible nodule structure from the images, besides the application of the LGD method to estimate the parameter of Gaussian distribution to further localize and segment lung nodules. This approach would benefit radiologists in their effort to rapidly and accurately identify lung cancer by increasing nodule identification. The originality of this work consists of combining LGD with other types of MRT, such as wavelet multi-scale morphological analysis (WMMA), for the improvement of Seg in nodules presented in CT images. In addition, the finer segmentation of features with the help of convolutional neural network (CNN) in the later stages does help overcome the issues regarding identification of lung nodule and thus offers better help to the radiologists in patient management systems.

The paper is structured as follows: section 2 reviews works related to the approach discussed. Section 3 presents the proposed method. Section 4 reviews the whole work. Lastly, section 5 gives the conclusion and future work.

2.   RELATED WORK

The following are the works that discuss the approaches and techniques of detecting and classifying lung nodules, for instance, deep learning, handcrafted features, multiscale, or 3D CNN. A hybrid machine learning method to predict the early prognosis of lung nodules using clinical images is presented in [10]. This procedure has three primary steps. First, an improved snake swarm optimization algorithm involving a bat model is implemented to segment the lung nodules accurately. The second step is selecting the best features to minimize dimensionality issues. A hybrid learning-based deep neural network is generated to predict and classify nodules.

The stages of detecting lung tumour regions are analyzed in [11]. For example, preprocessing, segmentation, and classification models are identified. The adaptive median filter is selected to determine the noise during preprocessing. The work elaborates on the simple n effective model based on the U-Net structure to separate and detect lung nodules faster. A commercially available computer-aided detection system is tested in [12]. This system utilizes deep learning algorithms trained to identify, classify, quantify, and track the growth of actionable pulmonary nodules on chest CTs. The retrospective cohort of the data of the routine clinical population is studied.

The use of deep learning in the CAD systems of lung nodule segmentation as a part of lung cancer CTs is debated in [13]. This work aims to create a reliable and accurate method to segment lung nodule regions in 3D. We devise a novel nested 3D fully connected CNN with residual unit structures and a new loss function to improve the segmentation accuracy. The algorithm for identifying nodules by comparing the multiple images is described in [14]. Generally, this technique provides more data for radiologists to facilitate early cancer detection. During the performance assessment process, such qualities as accuracy, precision and specificity are evaluated. The last CNN algorithm has decent precision, accuracy, and high specificity, which means it can minimize false positives due to intensive and frequent training. However, some obstacles remain, such as the size and character of the datasets, various nodule sizes and shapes, and the robustness of the CT scanner and acquisition protocol. Most recent research aims to improve the precision, efficacy and automation of the nodule detection, analysis and diagnosis process with the earlier stages of lung cancer.

3.   METHOD

In this section, the proposed method combines MRT [15], [16] and the LGD [17], [18] method to detect the nodules present in the lung CT images. It involves the following steps to enable smooth segmentation and detection as illustrated in Figure 1.

3.1. Data preprocessing

Preprocessing CT images is a critical first step that ensures optimal image quality for nodule detection. Specialized filtering techniques are applied to the raw CT data to reduce unwanted noise that could interfere with analysis. Image contrast is then carefully enhanced to better distinguish potential nodules from surrounding tissue while smoothing operations help eliminate artifacts and create more uniform regions for processing.

3.1.1. Noise reduction

Noise reduction technique is used to reduce the noise present in the CT images since it hinders the segmentation and detection of lung nodules. The research applies the conventional Gaussian smoothing [19],

[20] method, and this is defined as a weighted average of the pixels present in the CT image. The Gaussian smoothing is defined as in (1).

$$Ismoothed(x,y) = \frac{1}{16}\sum_{i=-1}^{1}\sum_{j=-1}^{1}\left(I(x+i,y+j)*G(i,j)\right) \qquad (1)$$

Where Ismoothed(x,y) is smoothed pixel value at (x, y)th position, I(x+i,y+j) is pixel value at (x+i, y+j)th position in the original image, and G(i,j) is Gaussian kernel weights at (i, j)th position. The research uses a 3×3 matrix as the Gaussian kernel that consists of a predetermined weights and this follows Gaussian distribution.
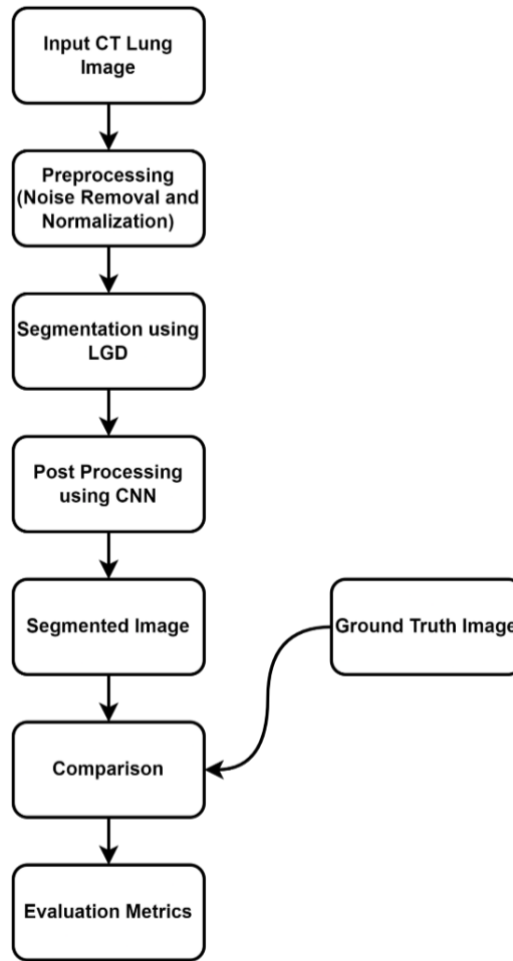

Figure 1. The flowchart of the proposed method

3.1.2. Contrast enhancement

This technique improves the contrast nature by reducing the difference between the contrast nature of various pixel regions in a CT image, which enables optimal identification of lung nodules. The research uses histogram equalization [21] to improve the contrast nature of a CT image and it is defined as in (2).

$$Ienhanced(x,y) = \left[\frac{(L-1)}{(M*N)}\right]*C(I(x,y)) \qquad (2)$$

Where Ienhanced(x, y) is enhanced pixel value at (x, y)th position, L is maximum intensity level (255 for 8-bit images), M and N is image dimension, and C(I(x, y) - cumulative histogram of a pixel till at (x, y)th position present in an original image.

Smoothing: smoothing techniques aim to reduce image noise and enhance the overall image quality. One commonly used smoothing technique is the mean filter, which replaces each pixel value with the average value of its neighboring pixels. The mean filtering is given in (3).

$$Ismoothed(x,y) = \frac{1}{(2k+1)^2} \sum_{i=-k}^{k} \sum_{j=-k}^{k} \big(I(x+i, y+j)\big) \tag{3}$$

Where Ismoothed(x, y) is smoothed pixel value at (x, y)th position, (2k+1) is smoothing kernel size (5×5).

3.2. Moving range analysis

During the lung nodule detection process, moving range (MR) analysis [22] improves the accuracy of the segmentation and detection. The subtle intensity variations and complex structures present in the CT images make the segmentation and detection of lung nodes challenging. The image decomposition into different levels uses the MR analysis, which provides a comprehensive image representation by capturing local and global details.

3.2.1. Wavelet analysis

Wavelet analysis [23] decomposes the CT-screened image into various frequency bands, which enables the identification of nodule structures present at different resolutions. The research uses discrete wavelet transform (DWT) as the vital technique to decompose the CT image into low-frequency approximation and high-frequency details. Thus, the DWT coefficients are expressed in (4) to (7).

Approximation coefficients for a scale j are expressed in (4).

$$Aj(x,y) = \frac{1}{\sqrt{2}} \sum_i \sum_j \big(h[i] * h[j] * I(2x-i, 2y-j)\big) \tag{4}$$

Horizontal detail coefficients for a scale j are expressed in (5).

$$Hj(x,y) = \frac{1}{\sqrt{2}} \sum_i \sum_j \big(g[i] * h[j] * I(2x-i, 2y-j)\big) \tag{5}$$

Vertical detail coefficients for a scale j are expressed in (6).

$$Vj(x,y) = \frac{1}{\sqrt{2}} \sum_i \sum_j \big(h[i] * g[j] * I(2x-i, 2y-j)\big) \tag{6}$$

Diagonal detail coefficients for a scale j are expressed in (7).

$$Dj(x,y) = \frac{1}{\sqrt{2}} \sum_i \sum_j \big(g[i] * g[j] * I(2x-i, 2y-j)\big) \tag{7}$$

Where h[i] is scaling filters, g[i] is wavelet filters, and I(2x-i, 2y-j) is pixel value at (2x-i, 2y-j)th position.

3.3. Multiscale morphological analysis

MMA improves [24] the detection of nodule structures by analyzing size, shape, and texture features at different orientations and scales. The morphological operations involving erosion (E) and dilation (D) are applied over the wavelet coefficients to refine nodule structure identification. These morphological operators are expressed in (8) and (9).

$$E(Aj, B) = \sum_i \sum_j \Big(min\, A_j\,(x+i, y+j), B(i,j)\Big) \tag{8}$$

$$D(Aj, B) = \sum_i \sum_j \Big(max\, A_j\,(x+i, y+j), B(i,j)\Big) \tag{9}$$

Where Aj is wavelet coefficients at scale j, B is structuring element, and (x+i, y+j) is wavelet coefficient position within a block.

3.4. Local Gaussian distribution method

In detecting lung nodules in CT screening images and LGD, the laterality orientation drawing evaluation test (LODET) method [17] is applied. This method is founded on estimating the statistics of the pixel intensities in the local blocks or regions assuming a Gaussian distribution. The mean and standard

deviation of the pixel intensity in each block can be calculated by translating lung nodules' corresponding probabilities of each place. In general, this method is to be used to detect and segment lung nodules. The CT image is then divided into blocks, and their local properties are estimated with the aid of a Gaussian distribution. Then, the predicted probabilities of a certain pixel belonging to a particular block are computed, and the pixel is sent to the nearest block in terms of probability [18].

Consequently, the lung nodules can be identified and segmented by assigning a probability of each pixel where each value is as close to one. This also enables us to identify lung nodules in more detail, categorise them, and distinguish them from the surrounding lung tissue and other visible structures, which is vital for radiologists to explore. This paper shows that one of the strengths of this method is the enhancement of the resolution of images and the use of approaches to enhance the efficiency of lung nodules' detection and early diagnosis of lung cancer. As a result, the LGD method is significant in lung nodule detection since it is based on local statistics and probability distribution to detect lung nodules and to make more objective judgments on the part of the radiologists.

3.4.1. Local Gaussian distribution estimation

Initially, the CT screening image is subdivided into smaller blocks or regions. The size of the blocks varies based on the CT image complexity. The objective of dividing the block enables the analysis of local image features and the estimation of Gaussian distribution parameters for each block.

The LGD method calculates the mean (μ) and standard deviation (σ) of the pixel intensities within each block B(x, y). The μ defines the average intensity level, whereas the σ indicates pixel intensity variation in a block. The Gaussian distribution parametric estimation is hence computed as in (10).

$$\mu(x,y) = \frac{1}{(w*h)} \sum_{i=1}^{w} \sum_{j=1}^{h} \big(B(x+i, y+j)\big)$$
$$\sigma(x,y) = \frac{1}{\sqrt{(w*h)}} \sum_{i=1}^{w} \sum_{j=1}^{h} \big(B(x+i, y+j) - \mu(x,y)\big)^2 \tag{10}$$

Where w is block width and h is block height.

3.4.2. Probability calculation

The pixel probability of a specific block in the CT image is estimated in this section. The pixel probability estimation shows that the pixel belonging to a specific block may reflect a lung nodule. Based on the Gaussian distribution parameter estimation, the probability calculation is given in (11).

$$P(x,y) = \frac{exp\big(-I(x,y) - \mu(x,y)\big)^2}{2*\sigma(x,y)^2} \tag{11}$$

Where I(x,y) is pixel intensity at (x, y)th position and P(x,y) is probability that quantifies the pixel intensity similarity with the Gaussian distribution in a block.

3.4.3. Segmentation

The LGD method concludes with segmentation, in which each pixel is assigned to the block with the highest probability. This step delimits the lung nodule borders, facilitating their subsequent localization and analysis. The process of segmentation is hence estimated in (12).

$$Isegmented(x,y) = B(argmax\ P(x,y)) \tag{12}$$

Where Isegmented(x,y) is segmented pixel value at at (x, y)th position and argmax P(x, y) is block position representing the maximum probability.

The LGD method calculates probabilities and performs segmentation of lung nodules by utilizing the estimated Gaussian distribution parameters within each block. Based on the highest probability, the blocks are assigned the pixels, where the segmentation method precisely defines the boundaries of nodules, allowing for their subsequent localization. LGD contributes to precise lung nodule characterization, facilitating early diagnosis and significantly improving patient outcomes.

3.5. Post-processing with residual dual attention CNN

Post-processing with residual dual attention (RDA)-CNN significantly refines the initial segmentation results to improve nodule detection accuracy. The residual connections in this architecture help preserve important spatial information throughout the deep network layers while mitigating the vanishing gradient problem. The dual attention mechanisms work in parallel to capture channel-wise and spatial

relationships in the feature maps, allowing the network to focus on the most relevant areas for nodule identification.

3.5.1. Residual connections

Residual connections are incorporated into the CNN to eradicate the vanishing gradient problem and enable a more uniform gradient flow during training. The skip connections find the residual mappings to effectively capture the segmented image data's details [25]. These architectural enhancements allow the network to learn deeper representations while maintaining computational efficiency and preventing degradation of training accuracy even in very deep networks.

3.5.2. Dual attention mechanisms

The dual attention mechanism improves CNN's ability to find relevant features by integrating both spatial and channel attention (CA) modules. The spatial attention (SA) module helps focus on important regions within each feature map by learning which areas contain the most useful information for nodule detection. Meanwhile, the CA module adaptively recalibrates channel-wise feature responses, emphasizing the most informative feature channels while suppressing less useful ones [26].

3.5.3. Spatial attention

The SA module [27] identifies the dependencies and spatial relationships within feature maps by assigning various attention weights to different spatial locations, highlighting the relevant regions and suppressing the irrelevant regions. Consider an input feature map F for a segmented image of size H×W×C of height (H), width (W), and channels (C). The SA computes the weights Aspatial as expressed in (13).

$$Aspatial = softmax(Conv2D(ReLU(Conv2D(F)))) \tag{13}$$

Where Conv2D is convolutional layer, rectified linear unit (ReLU) is rectified linear unit, and softmax is activation function for weight normalization.

CA: the CA module investigates the interdependencies between the feature channels by assigning the attention weights over the featured channels. This allows the CA to adapt dynamically to focus on the salient features in a channel. The CA computes the weights achannel for channel C as in (14).

$$Achannel = sigmoid(GlobalAvgPool2D(ReLU(Dense(GlobalAvgPool2D(F))))) \tag{14}$$

Where GlobalAvgPool2D is global average pooling operation and Dense is fully connected layer.

Figures 2 and 3 illustrates the attention-enhanced CNN architecture utilized in our research for robust feature extraction and segmentation in lung nodule detection. This architecture incorporates several key components: the RDA-CNN integrates spatial and CA mechanisms, enhancing the network's ability to focus on relevant features within the input data. The SA block selectively emphasizes informative spatial regions, while the CA block adjusts the importance of feature channels based on their relevance.

These blocks are integrated into a fusion and refinement stage, where features from different attention mechanisms are combined and further processed to enhance feature representation. The architecture culminates in a final convolutional layer, which produces output feature maps used for accurate segmentation of lung nodules. Figures 2 and 3 visually represents how these components interact to improve the segmentation performance by effectively leveraging attention mechanisms tailored for medical image analysis.
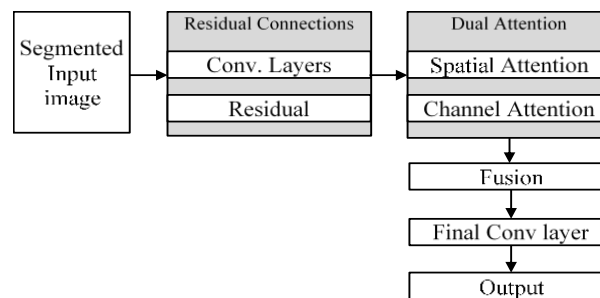

Figure 2. Architecture design: attention-enhanced CNN architecture for segmentation
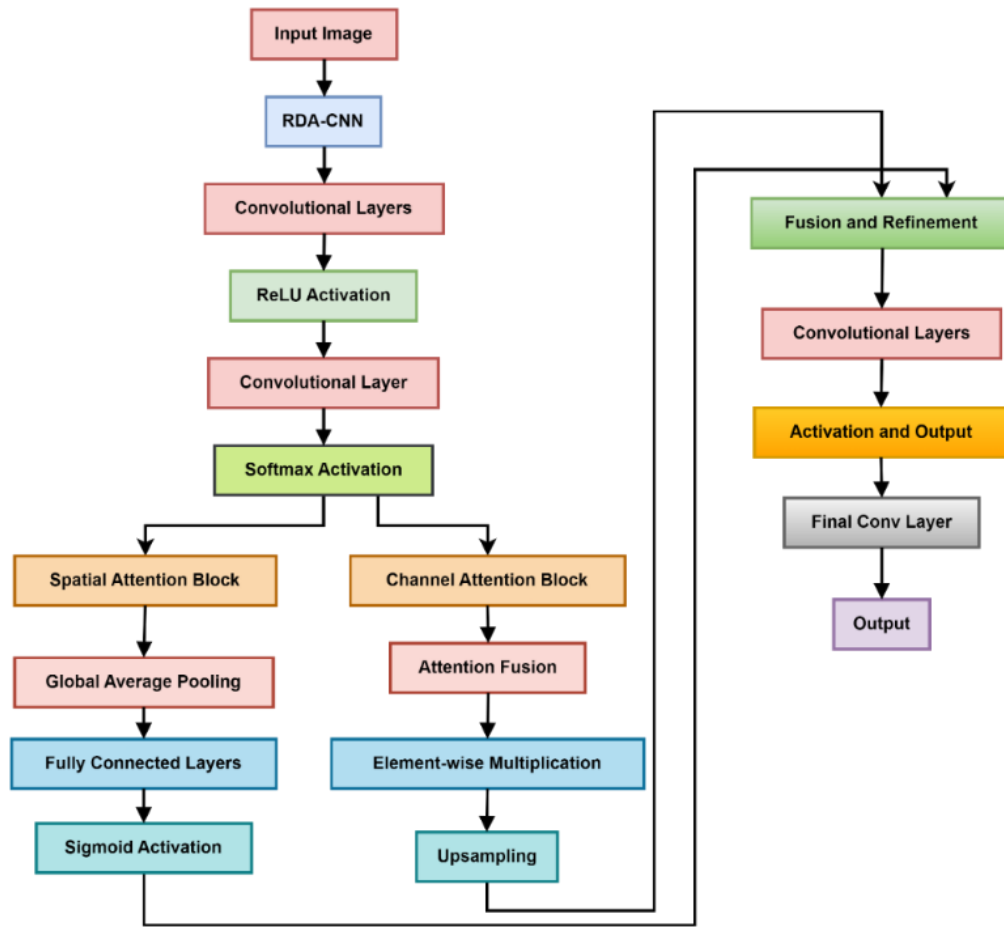
Figure 3. Architecture design: attention-enhanced CNN architecture for feature extraction

4. PERFORMANCE EVALUATION

In this section, the proposed method's performance is compared with other existing methods. The simulation is conducted in MATLAB, which runs on an i5-core processor with 8 GB of RAM. The performance of the proposed method is estimated in terms of accuracy, precision, recall, and F1-score.

4.1. Experimental setup

The data is collected from two publicly available datasets, including the lung image database consortium-image database resource initiative (LIDC-IDRI) and LUNA16 databases [28]. The database contains CT-scanned images with malignant/benign labels. The data is split into training, testing, and validation, where 70% is used for training, 15% for validation, and 15% for testing.

Table 1 summarizes key hyperparameters essential for training the segmentation and classification model in the proposed lung nodule detection system. These parameters include the learning rate of 0.001, batch size of 16, and 50 epochs for training convergence. A dropout rate of 0.2 helps prevent overfitting, while the Adam optimizer and dice loss function are chosen for efficient optimization and accurate segmentation evaluation, respectively. The model operates on 256×256 images with 32 filters for feature extraction, enhanced by an RDA mechanism and 16×16 block size for improved spatial context awareness.

Table 2 details simulation parameters crucial for the level set method used in lung nodule segmentation. It specifies 100 iterations and a time step of 100 for iterative refinement, along with a regularization parameter adjusted dynamically to 0.2 per time step. A scale parameter of 50 modulates sensitivity to spatial and intensity variations, optimizing segmentation accuracy. Additional parameters like computing gradient parameters, initial function settings $c_0 = 2$ and weighting factors ($\lambda_1 = 1$, $\lambda_2 = 1$) for foreground and background intensities ensure robust segmentation performance. Penalty and smoothness weighting parameters further fine-tune segmentation outputs for precise delineation of lung nodules in medical imaging.

Table 1. Hyperparameters for segmentation and classification

Hyperparameter	Value
Learning rate	0.001
Batch size	16
Number of epochs	50
Dropout rate	0.2
Optimizer	Adam
Loss function	Dice
Image size	256×256
Number of filters	32
Attention mechanism	RDA
Block size (LGD)	16×16

Table 2. Simulation parameters for LGD segmentation

Simulation parameter	Value
Iterations	100
Time step	100
Regularization parameter	0.2/time step
Scale parameter	50
Computing gradient parameter	1
Level set-initial function c0	2
λ_1 (foreground intensity weighting parameter)	1
λ_2 (background intensity weighting parameter)	1
Penalty parameter	0.001255255
Smoothness weighting parameter	20

4.2. Results and evaluation

In this section, the proposed method is tested individually on a new set of input images, where a sample of which is given in Figure 4. The results of the segmented region at various iterations are illustrated in Figure 4, and its respective segmented region is marked and shown, Figure 4(a) shows input image, Figure 4(b) shows 50th iteration, Figure 4(c) shows 100th iteration, Figure 4(d) shows 150th iteration, Figure 4(e) shows 200th iteration, and Figure 4(f) shows output image. Figure 5 shows that the loss is considerably reduced while segmenting an image using LGD and its associated total cost is highly reduced as in Figure 6. The evaluation metrics in Figure 7 show that the proposed method has higher accuracy, and precision, showing its viability in segmenting the relevant regions to find the nodules in the lung image.
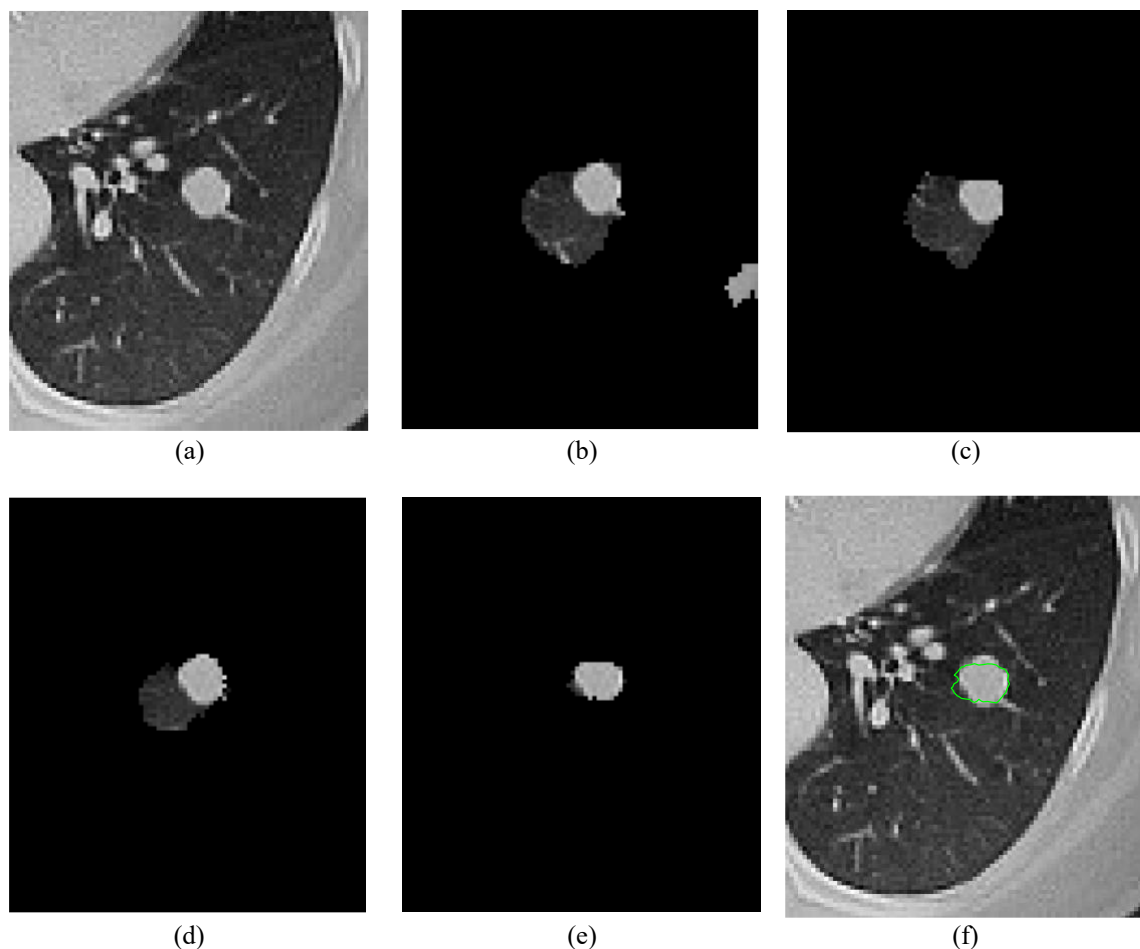

(a)   (b)   (c)

(d)   (e)   (f)

Figure 4. Identification of segmented regions at various stages of lung nodules of (a) input image, (b) 50th iteration, (c) 100th iteration, (d) 150th iteration, (e) 200th iteration, and (f) output image
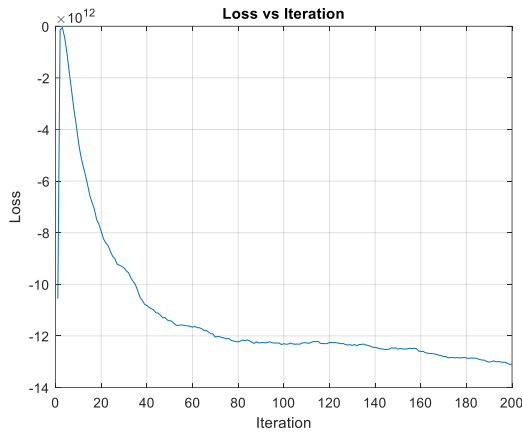
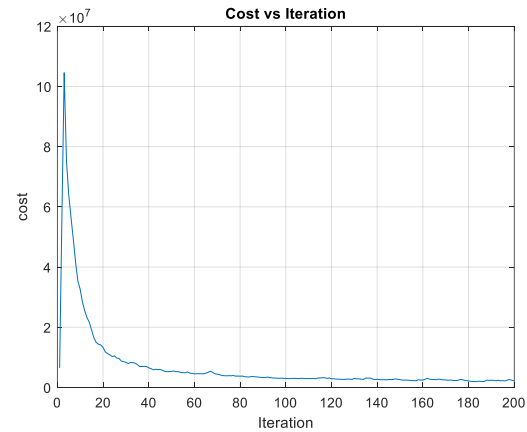Figure 5. Loss vs. iterations to segment the input image

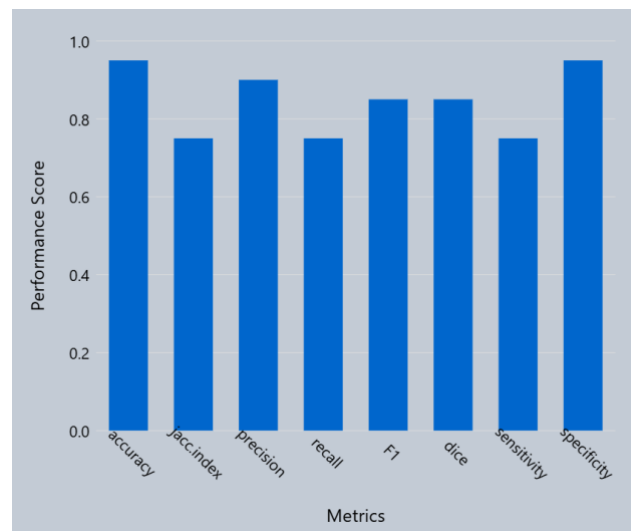Figure 6. Total cost vs. iterations to segment the input image

Figure 7. Evaluation metrics of the proposed method required to segment an input image

In this section, the comparative analysis is further conducted between the proposed method and various state-of-art methods. The performance is validated in terms of accuracy, precision, recall, and F1-measure. From the results of Table 3, it is found that the accuracy of the proposed method is higher accuracy across all test samples, with an average accuracy of 87.5%. Nested CNN performs second best, with an average accuracy of 83.6%. U-Net follows with an average accuracy of 81.5%. HL-DNN demonstrates the lowest accuracy, with an average of 78%.

From the results of Table 4, the proposed method consistently achieves higher precision across all test samples, with an average precision of 87.3%. Nested CNN performs second best, with an average precision of 84.2%. U-Net follows with an average precision of 81.9%. Health literacy-deep neural network (HL-DNN) demonstrates the lowest precision, with an average of 77.5%.

From the results of Table 5, the proposed method consistently achieves higher precision across all samples, with an average precision of 89.4%. Nested CNN performs second best, with an average precision of 86.2%. U-Net follows with an average precision of 84.7%. HL-DNN demonstrates the lowest precision, with an average of 79.7%.

From the results of Table 6, the proposed method consistently achieves higher F-measure across all samples, with an average F-measure of 88.3%. Nested CNN performs second best, with an average F-measure of 85.2%. U-Net follows with an average F-measure of 83.3%. HL-DNN demonstrates the lowest F-measure, with an average of 78.6%.

Table 3. Accuracy of various test CT screened image between the proposed method and existing state-of-art models

Test image sample	HL-DNN	U-Net	Nested CNN	Proposed method
10	75	78	80	85
20	76	79	81	86
30	77	80	82	86
40	77	81	82	87
50	78	81	83	87
60	78	82	84	88
70	79	82	85	88
80	79	83	86	88
90	80	84	86	89
100	81	85	87	90

Table 4. Precision of various test CT screened image between the proposed method and existing state-of-art models

Test image sample	HL-DNN	U-Net	Nested CNN	Proposed method
10	75	78	80	85
20	75	79	82	86
30	76	80	82	86
40	77	81	83	87
50	77	82	84	87
60	78	82	85	87
70	78	83	85	88
80	79	84	86	88
90	80	85	87	89
100	80	85	88	90

Table 5. Recall of various test CT screened image between the proposed method and existing state-of-art models

Test image sample	HL-DNN	U-Net	Nested CNN	Proposed method
10	77	81	82	87
20	78	82	84	88
30	78	83	84	88
40	79	84	85	89
50	80	85	86	89
60	80	85	87	90
70	80	86	87	90
80	81	86	88	90
90	82	87	89	91
100	82	88	90	92

Table 6. F-measure of various test CT screened image between the proposed method and existing state-of-art models

Test Image Sample	HL-DNN	U-net	Nested CNN	Proposed Method
10	76	79	81	86
20	76	80	83	87
30	77	81	83	87
40	78	82	84	88
50	78	83	85	88
60	79	83	86	88
70	79	84	86	89
80	80	85	87	89
90	81	86	88	90
100	81	86	89	91

5. CONCLUSION

This work has focused on designing and implementing an automated lung nodule detection system for use in CT screening images. The proposed system described the LGD method further than an RDA-CNN, using MRT, including wavelet and MMA. The presented approach confirmed that the established system can successfully detect and segment exogenous lung nodules. The classification accuracy, precision, and

F-measure were higher than the three existing methods. The mean of the proposed technique was 87.6%, which was higher than observed compared to other types of methods. Precision and F-measure values are consistently higher, which validate the finding of an improved ability to classify and segment lung nodules correctly. In future work, efforts could be dedicated to the use of larger databases that show improvement in the results; another question could be answered through clinical trials to ensure that the performance of the network, more so, the architecture of the network and other hyperparameters could be further refined to outdo the results proposed. However, incorporating other clinical characteristics and exploring possibilities could enhance the system's performance.

FUNDING INFORMATION

AUTHOR CONTRIBUTIONS STATEMENT
This journal uses the Contributor Roles Taxonomy (CRediT) to recognize individual author contributions, reduce authorship disputes, and facilitate collaboration.

Name of Author	C	M	So	Va	Fo	I	R	D	O	E	Vi	Su	P	Fu
Inbasakaran Govindan	✓	✓	✓	✓	✓	✓		✓	✓		✓			
Anitha Ruth Joseph Raj	✓	✓		✓	✓		✓			✓		✓	✓	

C	:	**C**onceptualization	I	:	**I**nvestigation	Vi	:	**Vi**sualization
M	:	**M**ethodology	R	:	**R**esources	Su	:	**Su**pervision
So	:	**So**ftware	D	:	**D**ata Curation	P	:	**P**roject administration
Va	:	**Va**lidation	O	:	Writing - **O**riginal Draft	Fu	:	**Fu**nding acquisition
Fo	:	**Fo**rmal analysis	E	:	Writing - Review & **E**diting			

CONFLICT OF INTEREST STATEMENT
The authors state no conflict of interest.

INFORMED CONSENT
We have obtained informed consent from all individuals included in this study.

DATA AVAILABILITY
Data availability is not applicable to this paper as no new data were created or analyzed in this study.

REFERENCES
[1] W. Cao, H. Da Chen, Y. W. Yu, N. Li, and W. Q. Chen, "Changing profiles of cancer burden worldwide and in China: A secondary analysis of the global cancer statistics 2020," *Chinese Medical Journal*, vol. 134, no. 7, pp. 783–791, 2021, doi: 10.1097/CM9.0000000000001474.
[2] N. Faruqui, M. A. Yousuf, M. Whaiduzzaman, A. K. M. Azad, A. Barros, and M. A. Moni, "LungNet: A hybrid deep-CNN model for lung cancer diagnosis using CT and wearable sensor-based medical IoT data," *Computers in Biology and Medicine*, vol. 139, 2021, doi: 10.1016/j.compbiomed.2021.104961.
[3] S. A. Khan *et al.*, "Lungs nodule detection framework from computed tomography images using support vector machine," *Microscopy Research and Technique*, vol. 82, no. 8, pp. 1256–1266, 2019, doi: 10.1002/jemt.23275.
[4] R. Li, C. Xiao, Y. Huang, H. Hassan, and B. Huang, "Deep learning applications in computed tomography images for pulmonary nodule detection and diagnosis: a review," *Diagnostics*, vol. 12, no. 2, 2022, doi: 10.3390/diagnostics12020298.
[5] T. Liu *et al.*, "Automated detection and classification of thyroid nodules in ultrasound images using clinical-knowledge-guided convolutional neural networks," *Medical Image Analysis*, vol. 58, 2019, doi: 10.1016/j.media.2019.101555.
[6] P. Sengodan, K. Srinivasan, R. Pichamuthu, and S. Matheswaran, "Early detection and classification of malignant lung nodules from CT images: An optimal ensemble learning," *Expert Systems with Applications*, vol. 229, 2023, doi: 10.1016/j.eswa.2023.120361.
[7] J. Li *et al.*, "Digital decoding of single extracellular vesicle phenotype differentiates early malignant and benign lung lesions," *Advanced Science*, vol. 10, no. 1, 2023, doi: 10.1002/advs.202204207.
[8] S. Vicini *et al.*, "A narrative review on current imaging applications of artificial intelligence and radiomics in oncology: focus on the three most common cancers," *Radiologia Medica*, vol. 127, no. 8, pp. 819–836, 2022, doi: 10.1007/s11547-022-01512-6.
[9] P. Dutande, U. Baid, and S. Talbar, "LNCDS: A 2D-3D cascaded CNN approach for lung nodule classification, detection and segmentation," *Biomedical Signal Processing and Control*, vol. 67, 2021, doi: 10.1016/j.bspc.2021.102527.
[10] A. S. Musthafa, K. Sankar, T. Benil, and Y. N. Rao, "A hybrid machine learning technique for early prediction of lung nodules from medical images using a learning-based neural network classifier," *Concurrency and Computation: Practice and Experience*, vol. 35, no. 3, 2023, doi: 10.1002/cpe.7488.

[11] M. Murugesan, K. Kaliannan, S. Balraj, K. Singaram, T. Kaliannan, and J. R. Albert, "A Hybrid deep learning model for effective segmentation and classification of lung nodules from CT images," *Journal of Intelligent and Fuzzy Systems*, vol. 42, no. 3, pp. 2667–2679, 2022, doi: 10.3233/JIFS-212189.

[12] J. T. Murchison *et al.*, "Validation of a deep learning computer aided system for CT based lung nodule detection, classification, and growth rate estimation in a routine clinical population," *PLoS ONE*, vol. 17, no. 5, 2022, doi: 10.1371/journal.pone.0266799.

[13] S. Kido *et al.*, "Segmentation of lung nodules on CT images using a nested three-dimensional fully connected convolutional network," *Frontiers in Artificial Intelligence*, vol. 5, 2022, doi: 10.3389/frai.2022.782225.

[14] I. Haq *et al.*, "Lung nodules localization and report analysis from computerized tomography (CT) scan using a novel machine learning approach," *Applied Sciences*, vol. 12, no. 24, 2022, doi: 10.3390/app122412614.

[15] T. Kavzoglu and H. Tonbul, "A comparative study of segmentation quality for multi-resolution segmentation and watershed transform," *Proceedings of 8th International Conference on Recent Advances in Space Technologies, RAST 2017*, pp. 113–117, 2017, doi: 10.1109/RAST.2017.8002984.

[16] L. Jianqing and Y.-H. Yang, "Multiresolution color image segmentation," *IEEE Transactions on Pattern Analysis and Machine Intelligence*, vol. 16, no. 7, pp. 689–700, 1994, doi: 10.1109/34.297949.

[17] L. Wang, J. Macione, Q. Sun, D. Xia, and C. Li, "Level set segmentation based on local Gaussian distribution fitting," *Computer Vision – ACCV 2009*, pp. 293–302, 2010, doi: 10.1007/978-3-642-12307-8_27.

[18] Y. Yu *et al.*, "Techniques and challenges of image segmentation: a review," *Electronics*, vol. 12, no. 5, 2023, doi: 10.3390/electronics12051199.

[19] M. Singh and S. Indu, "Denoising of palm leaf manuscripts using Gaussian filter and conservative smoothing," *AIP Conference Proceedings*, vol. 2521, 2023, doi: 10.1063/5.0142237.

[20] T. Hua, Q. Li, K. Dai, X. Zhang, and H. Zhang, "Image denoising via neighborhood-based multidimensional Gaussian process regression," *Signal, Image and Video Processing*, vol. 17, no. 2, pp. 389–397, 2023, doi: 10.1007/s11760-022-02245-9.

[21] M. Mehdizadeh, K. T. Tafti, and P. Soltani, "Evaluation of histogram equalization and contrast limited adaptive histogram equalization effect on image quality and fractal dimensions of digital periapical radiographs," *Oral Radiology*, vol. 39, no. 2, pp. 418–424, 2023, doi: 10.1007/s11282-022-00654-7.

[22] F. Zulfiqar, U. I. Bajwa, and Y. Mehmood, "Multi-class classification of brain tumor types from MR images using EfficientNets," *Biomedical Signal Processing and Control*, vol. 84, 2023, doi: 10.1016/j.bspc.2023.104777.

[23] Y. Yu, K. She, J. Liu, X. Cai, K. Shi, and O. M. Kwon, "A super-resolution network for medical imaging via transformation analysis of wavelet multi-resolution," *Neural Networks*, vol. 166, pp. 162–173, 2023, doi: 10.1016/j.neunet.2023.07.005.

[24] S. T. M. Ataky, D. Saqui, J. de Matos, A. d. S. B. Junior, and A. L. Koerich, "Multiscale analysis for improving texture classification," *Applied Sciences*, vol. 13, no. 3, 2023, doi: 10.3390/app13031291.

[25] W. Wu, S. Liu, Y. Xia, and Y. Zhang, "Dual residual attention network for image denoising," *Pattern Recognition*, vol. 149, 2024, doi: 10.1016/j.patcog.2024.110291.

[26] R. Padate, A. Jain, M. Kalla, and A. Sharma, "Image caption generation using a dual attention mechanism," *Engineering Applications of Artificial Intelligence*, vol. 123, 2023, doi: 10.1016/j.engappai.2023.106112.

[27] Q. Bao, Y. Liu, B. Gang, W. Yang, and Q. Liao, "SCTANet: a spatial attention-guided CNN-transformer aggregation network for deep face image super-resolution," *IEEE Transactions on Multimedia*, vol. 25, pp. 8554–8565, 2023, doi: 10.1109/TMM.2023.3238522.

[28] M. Palani, S. Rajagopal, and A. K. Chintanpalli, "A systematic review on feature extraction methods and deep learning models for detection of cancerous lung nodules at an early stage–the recent trends and challenges," *Biomedical Physics & Engineering Express*, vol. 11, no. 1, Jan. 2025, doi: 10.1088/2057-1976/ad9154.

BIOGRAPHIES OF AUTHORS

Mr. Inbasakaran Govindan is working as an Assistant Professor SRM Arts and Science College, Chennai with 15 years of teaching experience for UG and PG. Educational Qualification: M.Sc., M.Phil. His are of interest is social network analysis and data mining. He can be contacted at email: ginbasakaran@gmail.com.

Dr. Anitha Ruth Joseph Raj is working as Associate Professor in SRM Institute of Science and Technology, Chennai with 21 years of teaching experience for undergraduate and post graduate students in Department of Computer Science. She has a Doctorate degree in computer science and engineering from SRMIST. She also has completed her master degree and bachelor degree from University of Madras. She has published her papers over 7 international journals and has two filed patents, two text books and one book chapter to her credit. She is an editor for the book chapter "Innovative machine learning applications for cryptography", IGI Global Publisher. She is a member of Indian Science Congress. She has always enjoyed teaching and providing knowledge to the student from different forms of life. Her work experience involves in taking class, a counsellor to counsel the students to have a good career. Her research area includes deep learning, neural network and security. She can be contacted at email: anithaj@srmist.edu.in.